Metal-catalyzed reductive deamination of glutamic acid to bio-based dimethyl glutarate and methylamines

Free De Schouwer,[a] Thomas Cuypers,[a] Laurens Claes[a] and Dirk E. De Vos*[a]

[a] Centre for Surface Chemistry and Catalysis, Department of Microbial and Molecular Systems, KU Leuven - University of Leuven, Celestijnenlaan 200F, Post Box 2461, 3001 Heverlee, Belgium. E-mail: dirk.devos@kuleuven.be

Supporting Information

1. General

1.1 Chemicals

L-Glutamic acid (Acros Organics, 99%), γ-carboxy-γ-butyrolactone (Sigma Aldrich, 98%), dimethyl glutarate (Sigma Aldrich, 99%), dimethyl adipate (Sigma Aldrich, ≥ 99%), methanol (Fisher Scientific, 99%), formaldehyde (Sigma Aldrich, 37% in water), acetyl chloride (Janssen Chimica, 98%), *N*,*N*-dimethylcyclohexylamine (Sigma Aldrich, 99%), α-ketoglutaric acid (Sigma Aldrich, 99%), deuterium oxide (Sigma Aldrich, 99.9%) were all used as received. Catalysts were prepared from metal precursors and supports: $Pt(NH_3)_4Cl_2{\cdot}H_2O$ (Sigma Aldrich, ≥ 99.99%), $Pd(NH_3)_4Cl_2{\cdot}H_2O$ (Sigma Aldrich, ≥ 99.99%), $RuCl_3{\cdot}H_2O$ (Acros Organics, 35-40% Ru), $RhCl_3{\cdot}H_2O$ (ABCR, 38.5-45.5%), SiO_2 (Evonik, Aerosil 380), Al_2O_3 (acidic, CONDEA Chemie, Puralox NGa-150), Al_2O_3 (basic, Sigma Aldrich), TiO_2 (Alfa Aesar, catalyst support 1/8" pellets, anatase), ZrO_2 (Alfa Aesar, catalyst support 1/8" pellets), SiO_2-Al_2O_3 (Grace Silica GmbH, 13% Al_2O_3). Commercial catalysts include 5 wt% Pt/C (Johnson Matthey), 5 wt% Pd/C (Johnson Matthey), 5 wt% Ru/C (Alfa Aesar) and 5 wt% Rh/C (Johnson Matthey).

1.2 Synthesis of *N*,*N*-dimethylglutamic acid, *N*,*N*-dimethylaspartic acid and dimethyl *N*,*N*-dimethylglutamate

N,*N*-Dimethylglutamic acid and *N*,*N*-dimethylaspartic acid were synthesized according to an adapted synthesis procedure.[1] A 50 ml high-pressure Parr batch reactor (Series 5500; Type SS-316; Model 4848 temperature controller) was charged with L-glutamic acid or L-aspartic acid (0.01 mol), formaldehyde (0.022 mol, 37 wt% in water), 5 wt% Pd/C (0.9 mol% Pd) and water (20 ml). The reactor was sealed, purged 3 times with N_2, 3 times with H_2 and finally pressurized with 40 bar H_2. Next, the reactor was heated to 50 °C and stirred vigorously (830 rpm). After 3 h, the reactor was cooled down to room temperature in an ice bath, the pressure was released and the solid catalyst was removed by centrifugation. Next, water, methanol (originating from the hydrogenation of formaldehyde) and residual formaldehyde were evaporated under vacuum. The solid product was dried at 60 °C overnight and analyzed with ^{1}H-NMR spectroscopy.

An analogous procedure was used to synthesize dimethyl *N*,*N*-dimethylglutamate starting from dimethyl-L-glutamate hydrochloride. Dimethyl *N*,*N*-dimethylglutamate was purified by dissolving the crude solid product in water (10 ml), together with a small excess of sodium hydroxide, and extracting with diethyl ether (10 x 10 ml).

The organic phases were combined, dried with magnesium sulfate and diethyl ether was evaporated under a gentle N_2-flow. The purified liquid product was analyzed with ^{1}H-NMR spectroscopy and GC-MS.

1.3 Product analysis and identification

The purity of *N*,*N*-dimethylglutamic acid and *N*,*N*-dimethylaspartic acid was verified by ^{1}H-NMR spectroscopy. To that end, 300 µl of the aqueous reaction mixture or 6 mg of the purified product were mixed with respectively 300 µl or 600 µl D_2O in an NMR tube. ^{1}H-NMR spectra were recorded on a Bruker Avance 400 MHz spectrometer equipped with a BBO 5 mm atma probe and a sample case. When water was present, the broad signal around δ = 4.7 ppm was suppressed by applying an adapted zgpr pulse program: p1 9.75 µs; plw1 15W; plw9 5.7-05W; o1P on the resonance signal of water, determined and selected automatically.

Product quantification of deamination reactions was performed with gas chromatography (GC) by using dimethyl adipate as an external standard. For dimethyl glutarate and dimethyl *N*,*N*-dimethylglutamate calibration curves were made to determine the appropriate response factors. In case of other reaction products, response factors were calculated by using the effective carbon number of the different compounds:[2–5] ECN dimethyl glutarate = 4.4, ECN dimethyl *N*,*N*-dimethylglutamate = 5.65, ECN dimethyl α-methoxyglutarate = 4.4, ECN dimethyl α-hydroxyglutarate = 3.65, ECN γ-methoxycarbonyl-γ-butyrolactone = 3 and ECN dimethyl adipate = 5.47. The reaction mixture was analyzed by using a Shimadzu 2010 GC equipped with a DB-FFAP capillary column and a flame ionization detector (FID). An optimized temperature program allowed baseline separation of all compounds: column temperature was increased from 70 °C to 110 °C at 4 °C min^{-1}, kept constant for 60 min and increased further to 250 °C at 15 °C min^{-1} and finally a dwell time of 10 min was applied.

When water was used as the solvent, additional esterification was needed in order to perform GC analysis. Esterification was preceded by adding adipic acid (0.1 mmol) as an internal standard to the reaction mixture (1 ml) in a glass vial. Water was evaporated; the residue was dissolved in 1 ml methanol and acetyl chloride (0.4 mmol) was added while the recipient was cooled on ice. Next, the solution was stirred and heated to 70 °C for 1 h. The reaction was quenched by cooling the recipient on ice. Afterwards, excess reagents were evaporated under a gentle N_2-flow. Finally, the liquid residue was dissolved in methanol (1 ml) and analyzed with GC. Product identification was performed using gas chromatography coupled to a mass spectrometer (GC-MS), using an Agilent 6890 GC, provided with an HP-5 ms column and coupled to a 5973 MSD mass spectrometer.

1.4 Product identification

***N*,*N*-Dimethylglutamic acid (MW = 175 g mol^{-1})**

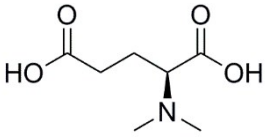

^{1}H-NMR (400 MHz, D_2O): 3.55 (dd, ^3J = 4.25 Hz, ^3J = 9.44 Hz, 1H; ($N(CH_3)_2$)($-CH_2$)>C**H**-COOH), 2.84 (s, 6H; -N(C**H**$_3$)$_2$), 2.46 (m, 2H; HOOC-C**H**$_2$-CH_2), 2.20 (m, 1H; -CH_2-HC**H**-CH<($N(CH_3)_2$)(COOH)), 1.96 (m, 1H; -CH_2-**H**CH-CH<($N(CH_3)_2$)(COOH)).

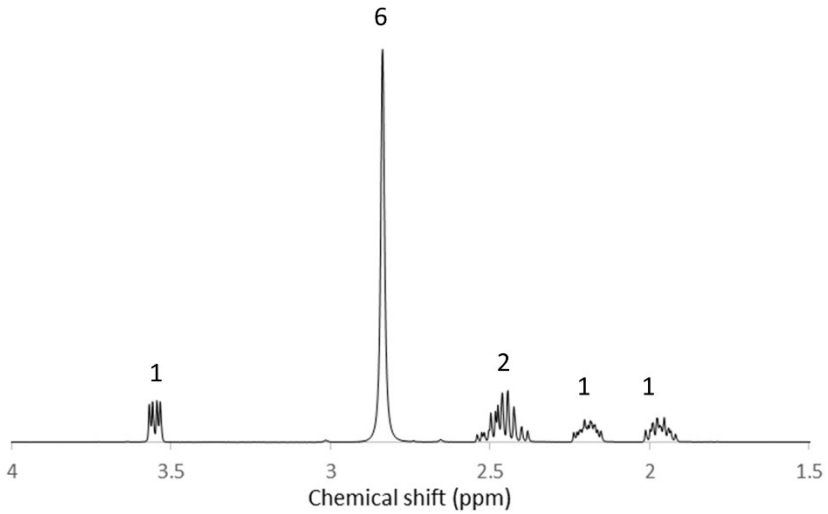

Figure S1. ^{1}H-NMR spectrum (400 MHz, D_2O) of *N*,*N*-dimethylglutamic acid.

***N*,*N*-Dimethylaspartic acid (MW = 161 g mol^{-1})**

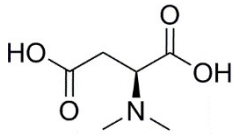

^{1}H-NMR (400 MHz, D_2O): 4.05 (t, ^{3}J = 5.76 Hz, 1H; $(N(CH_3)_2)(-CH_2)>C\underline{\mathbf{H}}$-COOH), 2.97 (t, ^{3}J = 5.76 Hz, 2H; HOOC-C$\underline{\mathbf{H}}_2$-), 2.87 (s, 6H; -N(C$\underline{\mathbf{H}}_3)_2$)

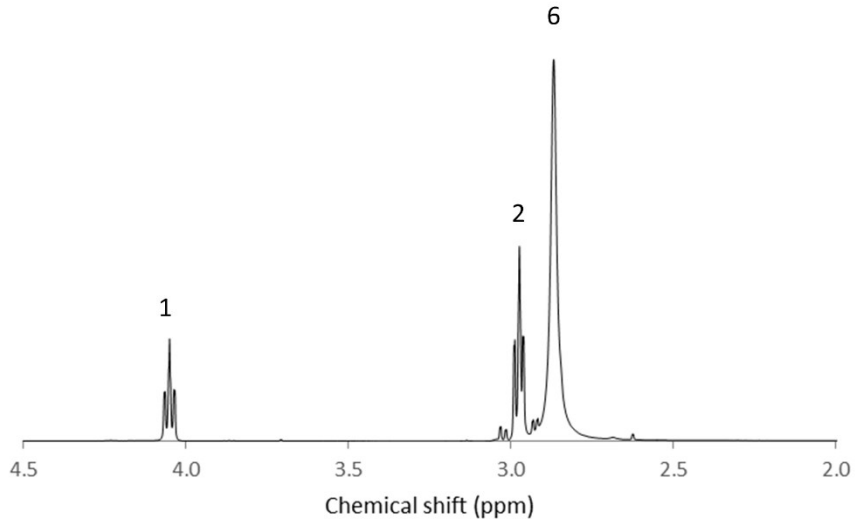

Figure S2. ^{1}H-NMR spectrum (400 MHz, D_2O) of *N*,*N*-dimethylaspartic acid.

Dimethyl glutarate (MW = 160 g mol^{-1})

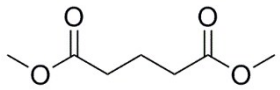

GC/MS (EI, 70 eV): m/z (rel. int., %): 130 (6), 129 (90), 128 (46), 102 (5), 101 (100), 97 (7), 87 (15), 85 (8), 72 (5), 59 (58), 55 (19), 43 (7), 42 (16), 41 (11), 39 (8).

Dimethyl *N*,*N*-dimethylglutamate (MW = 203 g mol^{-1})

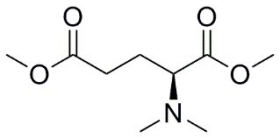

^{1}H-NMR (400 MHz, D_2O): 3.67 (s, 3H; $(N(CH_3)_2)(-CH_2)>CH-COOC\underline{\mathbf{H}}_3$), 3.61 (s, 3H; $\underline{\mathbf{H}}_3COOC-CH_2$-), 3.15 (t, ^{3}J = 7.37 Hz, 1H; $(N(CH_3)_2)(-CH_2)>C\underline{\mathbf{H}}-COOCH_3$), 2.34 (t, ^{3}J = 7.71 Hz, 2H; $H_3COOC-C\underline{\mathbf{H}}_2$-), 2.19 (s, 6H; $-N(C\underline{\mathbf{H}}_3)_2$), 1.94 (m, 2H; $-CH_2-C\underline{\mathbf{H}}_2-CH<(N(CH_3)_2)(COOCH_3)$)

GC/MS (EI, 70 eV): m/z (rel. int., %): 203 (1), 172 (7), 145 (8), 144 (100), 116 (7), 85 (5), 84 (47), 42 (5).

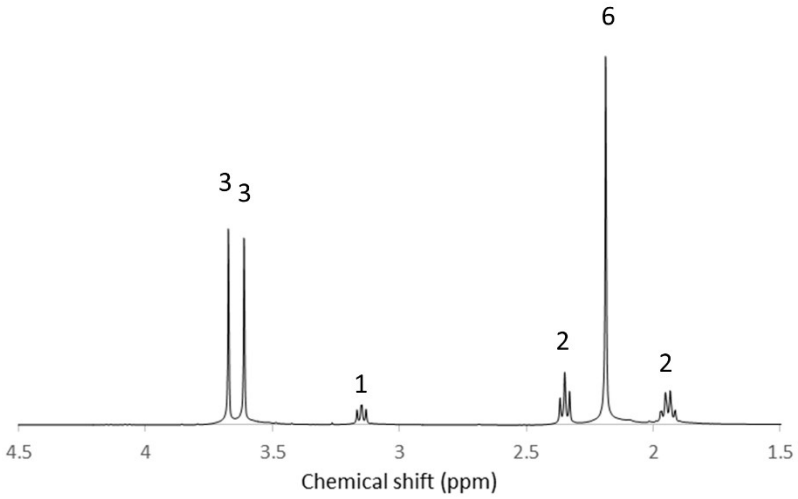

Figure S3. ^{1}H-NMR spectrum (400 MHz, D_2O) of dimethyl *N*,*N*-dimethylglutamate.

Methylamine (MW = 31 g mol^{-1})

GC/MS (EI, 70 eV): m/z (rel. int., %): 31 (57), 30 (100), 29 (17), 28 (77), 27 (12).

Dimethylamine (MW = 45 g mol^{-1})

GC/MS (EI, 70 eV): m/z (rel. int., %): 45 (55), 44 (100), 43 (10), 41 (7), 30 (7).

Trimethylamine (MW = 59 g mol^{-1})

GC/MS (EI, 70 eV): m/z (rel. int., %): 59 (49), 58 (100), 57 (6), 43 (11), 42 (55), 41 (11), 40 (8), 30 (15).

Dimethyl α-methoxyglutarate (MW = 190 g mol^{-1})

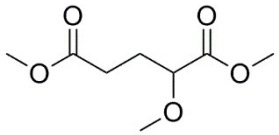

GC/MS (EI, 70 eV): m/z (rel. int., %): 132 (7), 131 (100), 115 (7), 99 (23), 72 (6), 71 (82), 59 (6), 41 (6).

Dimethyl α-hydroxyglutarate (MW = 176 g mol^{-1})

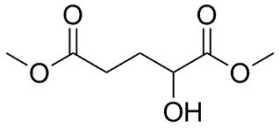

GC/MS (EI, 70 eV): m/z (rel. int., %): 145 (5), 117 (26), 86 (5), 85 (100), 59 (5), 57 (11).

γ-Methoxycarbonyl-γ-butyrolactone or methyl 5-oxotetrahydrofuran-2-carboxylate (MW = 144 g mol^{-1})

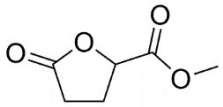

GC/MS (EI, 70 eV): m/z (rel. int., %): 144 (2), 86 (5), 85 (100), 59 (5), 57 (9), 39 (4).

Methyl *N*-methylpyroglutamate or methyl 5-oxopyrrolidine-2-carboxylate (MW = 157 g mol^{-1})

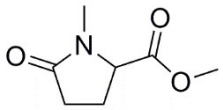

GC/MS (EI, 70 eV): m/z (rel. int., %): 157 (6), 99 (6), 98 (100), 70 (11), 68 (6), 42 (13), 41 (7).

***N*-Methylpyrrolidone (MW = 99 g mol^{-1})**

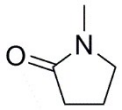

GC/MS (EI, 70 eV): m/z (rel. int., %): 99 (100), 98 (7), 71 (5), 70 (10), 56 (5), 44 (23), 43 (10), 41 (34), 41 (17), 40 (5), 39 (10).

γ-Butyrolactone (MW = 86 g mol^{-1})

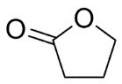

GC/MS (EI, 70 eV): m/z (rel. int., %): 86 (54), 85 (20), 57 (9), 56 (29), 55 (11), 42 (100), 41 (60), 40 (21), 39 (24), 38 (7).

Methyl γ-methoxybutyrate (MW = 132 g mol^{-1})

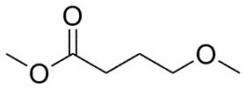

GC/MS (EI, 70 eV): m/z (rel. int., %): 117 (10), 116 (9), 102 (11), 101 (67), 100 (18), 87 (6), 86 (5), 85 (15), 74 (65), 72 (15), 71 (17), 69 (36), 59 (85), 58 (8), 57 (6), 56 (9), 55 (5), 45 (100), 43 (21), 42 (7), 41 (32), 39 (16).

Methyl γ-hydroxybutyrate (MW = 118 g mol^{-1})

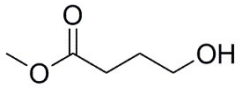

GC/MS (EI, 70 eV): m/z (rel. int., %): 89 (5), 88 (100), 87 (85), 86 (6), 85 (10), 75 (5), 74 (98), 69 (24), 60 (5), 59 (36), 58 (5), 57 (53), 56 (14), 56 (5), 55 (21), 45 (15), 44 (5), 43 (40), 42 (7), 41 (9), 40 (26), 39 (12).

2. Characterization of the catalyst support materials

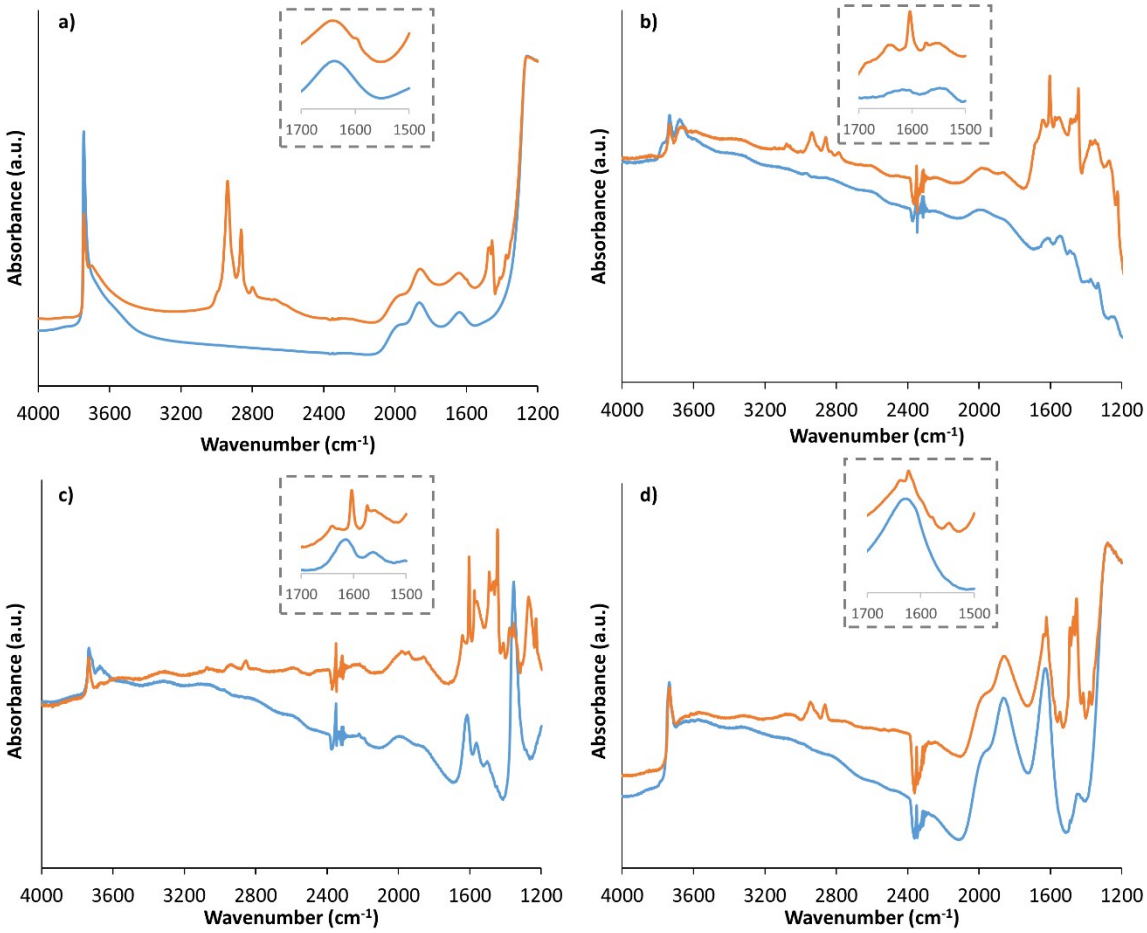

Figure S4. Reference FTIR spectra of self-supporting wafers of SiO_2 (**a**), ZrO_2 (**b**), TiO_2 (**c**) and SiO_2-Al_2O_3 (**d**) at 50 °C after activation at 400 °C (blue) and after adsorption of *N*,*N*-dimethylcyclohexylamine (orange). *N*,*N*-Dimethylcyclohexylamine (20 mbar) was allowed to adsorb at 50 °C and after saturation the samples were evacuated for 30 min to remove physisorbed probe molecules.

Note that specific interactions between *N*,*N*-dimethylcyclohexylamine and Lewis acid sites were difficult to designate; however, the ZrO_2 and TiO_2 supports used in this work have earlier been extensively characterized with pyridine FTIR, and were described as predominantly Lewis acidic.[6] Note that even weak Brønsted acid sites can be detected in our experiments because of the stronger basicity of *N*,*N*-dimethylcyclohexylamine compared to pyridine.

Table S1. Textural characterization of the support materials.

Entry	Support	S_{BET} (m^2 g^{-1}) [a]
1	SiO_2	380
2	ZrO_2	50
3	TiO_2	150
4	SiO_2-Al_2O_3	475
5	Al_2O_3 (acidic)	150

[a] *Brunauer-Emmett-Teller surface area.*

3. C-N Hydrogenolysis of *N*,*N*-dimethylglutamic acid in water: optimization of reaction conditions

Table S2. C-N Hydrogenolysis of *N*,*N*-dimethylglutamic acid in water using basic Pt/Al_2O_3: optimization of reaction parameters.[a]

Entry	H_2 pressure (bar)	Additive	Glutaric acid yield (%) [b]	Main amine product [c]
1	30	/	37	DMA
2	15	/	**49**	DMA
3	8	/	10	DMA
4	30	0.1 M H_3PO_4	24	TMA
5	30	0.05 M H_3PO_4	33	DMA
6	30	0.1 M NaOH	5	TMA

[a] *Conditions*: *N*,*N*-dimethylglutamic acid (0.1 M in water, 10 ml), basic Pt/Al_2O_3 (5 mol% Pt), additive, 200 °C, 24 h. [b] The conversion of *N*,*N*-dimethylglutamic acid was always > 99%. [c] DMA: dimethylamine; TMA: trimethylamine.

4. C-N Hydrogenolysis of *N*,*N*-dimethylglutamic acid in methanol: catalyst screening

Table S3. C-N Hydrogenolysis of *N*,*N*-dimethylglutamic acid in methanol: catalyst screening.[a]

Entry	Metal	Support	Temperature (°C)	Conversion (%)	Yield DMG (%) [b]	Yield DM α-OH-G + MCBL (%) [b]	Yield DM α-OCH_3-G (%) [b]	Yield others (%) [b]
1	Pt	C	200	100	52	17	2	29
2	Pt	C	225	100	73	0	3	24
3	Pt	SiO_2	200	96	19	42	13	22
4	Pt	SiO_2	225	100	16	41	24	29
5	Pt	Al_2O_3(acidic)	200	89	27	29	18	15
6	Pt	Al_2O_3(acidic)	225	100	35	14	35	16
7	Pt	Al_2O_3(basic)	200	88	20	42	20	6
8	Pt	Al_2O_3(basic)	225	100	58	5	18	19
9	Pt	SiO_2-Al_2O_3	200	96	32	44	14	6
10	Pt	SiO_2-Al_2O_3	225	100	39	20	26	15
11	Pt	ZrO_2	200	90	45	31	14	0
12	Pt	ZrO_2	225	100	71	0	12	17
13	Pt	TiO_2	200	99	67	11	2	19
14	Pt	TiO_2	225	100	76	2	8	14
15	Pd	C	200	99	3	58	7	31
16	Pd	C	225	100	18	18	22	42

17	Pd	SiO_2	200	86	4	52	10	20
18	Pd	SiO_2	225	100	2	54	27	17
19	Pd	Al_2O_3(acidic)	200	79	2	32	24	18
20	Pd	Al_2O_3(acidic)	225	100	8	26	34	32
21	Pd	ZrO_2	200	92	5	56	21	10
22	Pd	ZrO_2	225	100	7	30	31	32
23	Pd	TiO_2	200	99	4	64	8	23
24	Pd	TiO_2	225	100	21	15	31	33
25	Ru	C	200	98	55	15	6	22
26	Ru	C	225	100	63	0	10	27
27	Ru	SiO_2	200	100	13	53	10	24
28	Ru	SiO_2	225	100	32	20	23	25
29	Ru	Al_2O_3(acidic)	200	90	21	44	20	5
30	Ru	Al_2O_3(acidic)	225	100	25	27	23	25
31	Ru	SiO_2-Al_2O_3	200	89	23	40	10	16
32	Ru	SiO_2-Al_2O_3	225	100	28	21	15	36
33	Ru	ZrO_2	200	89	33	29	18	9
34	Ru	ZrO_2	225	100	39	17	24	20
35	Ru	TiO_2	200	95	32	41	16	6
36	Ru	TiO_2	225	100	34	14	25	27
37	Rh	C	225	100	62	2	8	28
38	Rh	SiO_2	200	86	12	46	23	5
39	Rh	SiO_2	225	100	28	29	27	16
40	Rh	Al_2O_3(acidic)	200	97	4	65	13	15
41	Rh	Al_2O_3(acidic)	225	100	3	35	36	26
42	Rh	ZrO_2	200	88	32	31	15	10
43	Rh	ZrO_2	225	100	34	12	28	26
44	Rh	TiO_2	200	96	7	57	17	15
45	Rh	TiO_2	225	100	20	21	36	23

[a] *Conditions*: *N*,*N*-dimethylglutamic acid (0.1 M in methanol, 10 ml), catalyst (5 mol% metal, 5 wt% metal on support), H_2 (30 bar), 24 h. [b] DMG: dimethyl glutarate; DM α-OH-G: dimethyl α-hydroxyglutarate; MCBL: γ-methoxycarbonyl-γ-butyrolactone; and DM α-OCH_3-G: dimethyl α-methoxyglutarate. Others: γ-butyrolactone, methyl γ-hydroxybutyrate, methyl γ-methoxybutyrate and non-identified, lower molecular weight compounds.

5. Kinetic experiments

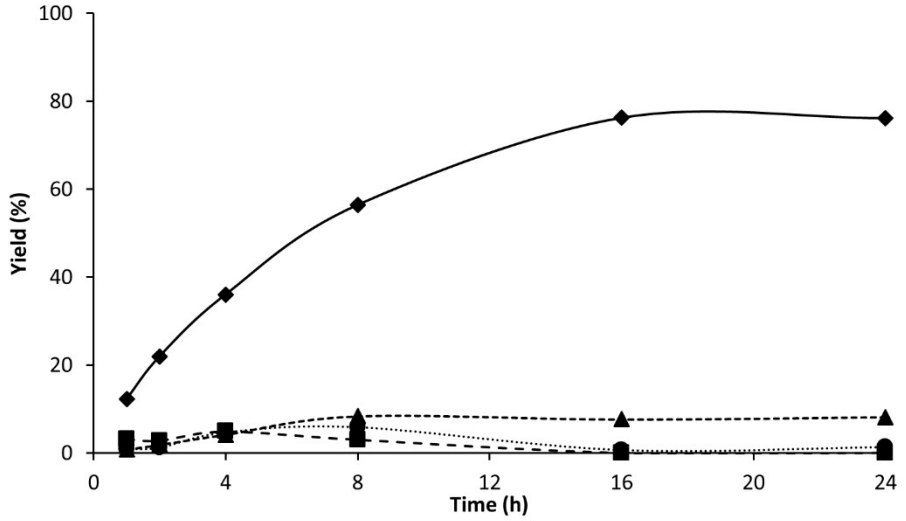

Figure S5. Catalytic C-N hydrogenolysis using 5 wt% Pt/TiO_2 as a function of time. *Conditions*: *N*,*N*-dimethylglutamic acid (0.1 M in methanol, 10 ml), catalyst (5 mol% Pt), H_2 (30 bar), 225 °C. Legend: dimethyl glutarate (◴), dimethyl α-hydroxyglutarate (O), γ-methoxycarbonyl-γ-butyrolactone (ᔓ) and dimethyl α-methoxyglutarate (□).

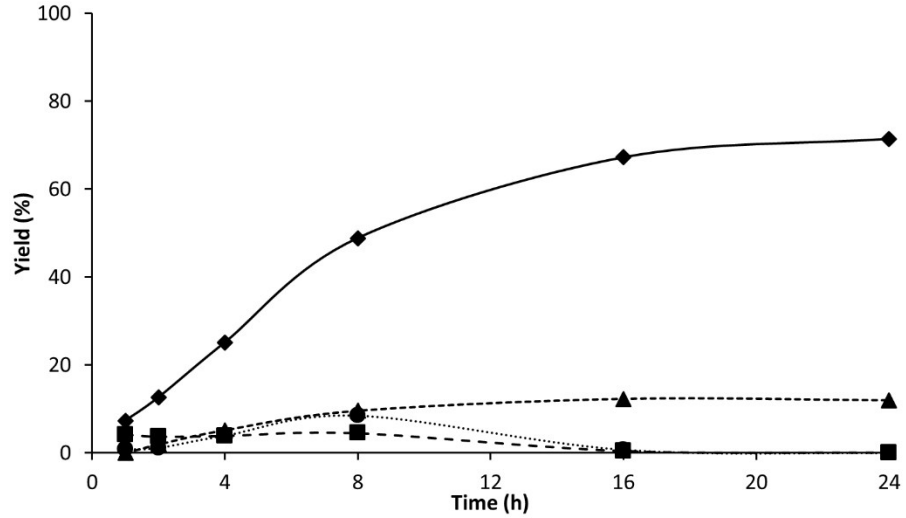

Figure S6. Catalytic C-N hydrogenolysis using 5 wt% Pt/ZrO_2 as a function of time. *Conditions*: *N*,*N*-dimethylglutamic acid (0.1 M in methanol, 10 ml), catalyst (5 mol% Pt), H_2 (30 bar), 225 °C. Legend: dimethyl glutarate (◴), dimethyl α-hydroxyglutarate (O), γ-methoxycarbonyl-γ-butyrolactone (ᔓ) and dimethyl α-methoxyglutarate (□).

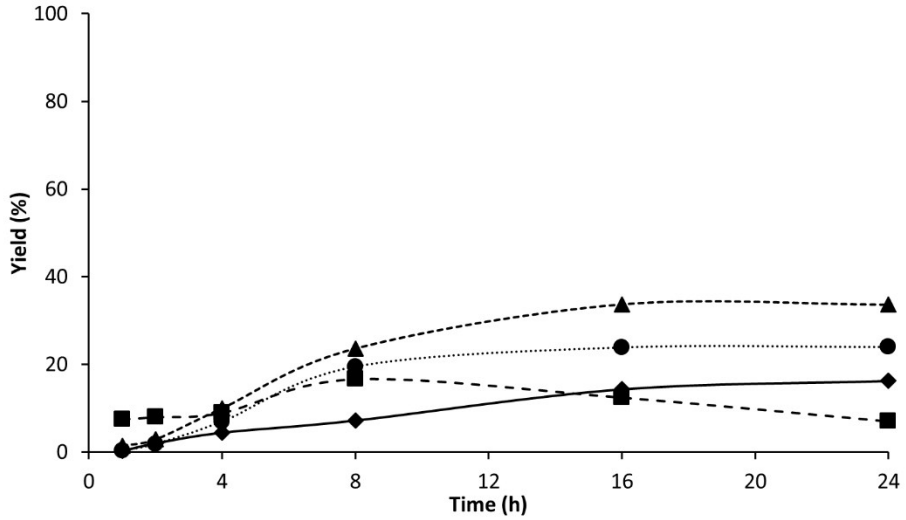

Figure S7. Catalytic C-N hydrogenolysis using 5 wt% Pt/SiO_2 as a function of time. *Conditions*: *N*,*N*-dimethylglutamic acid (0.1 M in methanol, 10 ml), catalyst (5 mol% Pt), H_2 (30 bar), 225 °C. Legend: dimethyl glutarate (◴), dimethyl α-hydroxyglutarate (O), γ-methoxycarbonyl-γ-butyrolactone (ꟽ) and dimethyl α-methoxyglutarate (□).

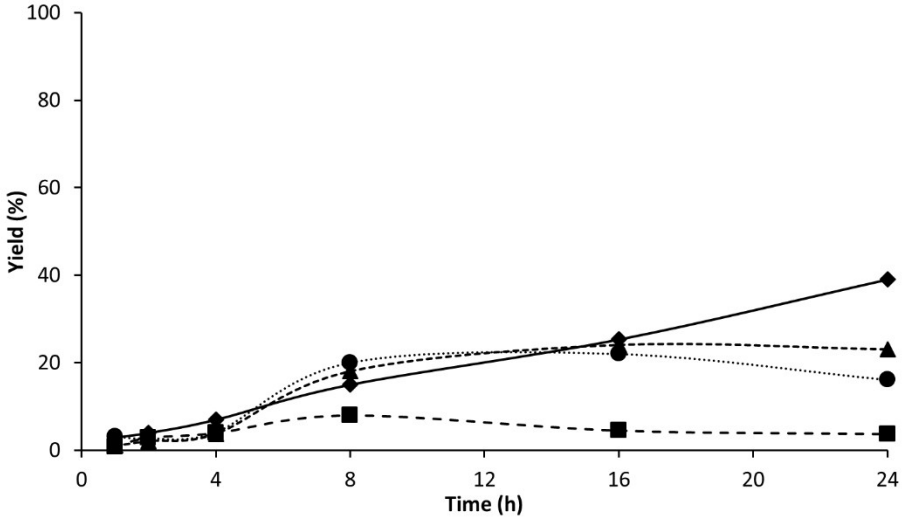

Figure S8. Catalytic C-N hydrogenolysis using 5 wt% Pt/SiO_2-Al_2O_3 as a function of time. *Conditions*: *N*,*N*-dimethylglutamic acid (0.1 M in methanol, 10 ml), catalyst (5 mol% Pt), H_2 (30 bar), 225 °C. Legend: dimethyl glutarate (◴), dimethyl α-hydroxyglutarate (O), γ-methoxycarbonyl-γ-butyrolactone (ꟽ) and dimethyl α-methoxyglutarate (□).

6. Effect of water

The fact that the formation of water has an effect on the initial selectivity has been shown. However, it is not yet clear whether water will slow down or maybe increase the rate of dimethyl glutarate formation, as the latter is a consecutive product of dehydration or C-O hydrogenolysis of dimethyl α-hydroxyglutarate. Therefore, the C-N hydrogenolysis of *N*,*N*-dimethylglutamic acid was performed in a 90/10 (v/v) solution of methanol/water. After 8 h, the conversion was 99% and the reaction mixture was composed of dimethyl glutarate (41%), dimethyl α-methoxyglutarate (9%) and hydrolysis products (33%). Besides the expected products, however, methyl *N*-methylpyroglutamate was obtained in 13% yield. The presence of water generates a lot of hydrolysis products and more MMA, which can induce the formation of methyl *N*-methylpyroglutamate as a stable end product. Although

the conversion was 12% higher compared to the reaction in pure methanol, dimethyl glutarate was obtained in much lower yield (41% *versus* 56%).

7. Economic feasibility study

The market price of low-quality protein-rich biomass streams, such as dried distillers grains with solubles (DDGS), sugar beet and sugar cane vinasses, soy bean, rapeseed and castor press cakes, slaughter waste, varies between 100-300 €/ton and depends on the protein content and properties (Table S4). So far, these side streams are processed into animal feed or combusted because of inherent toxicity (castor ricin protein) or microbial contamination (slaughter waste). Moreover, it has been estimated that the amount of protein waste will increase with 100 Mton per year if 25% of the transportation fuels would be replaced by biofuels in Europe by 2030.[7] Consequently, the generation of protein waste will exceed the current demands and hence, the market price of protein waste is expected to decrease even more. Since DDGS and vinasses typically contain a substantial amount of non-essential amino acids, in particular glutamic acid and aspartic acid, which have no significant value in animal feed formulation, new applications should be designed. For instance, the acidic amino acids can be isolated selectively by electrodialysis and processed further into bio-based chemicals. The other fraction, enriched in essential amino acids, will hence have a higher intrinsic value for feed applications.[8]

To illustrate the relevance of valorization of protein waste, economic feasibility calculations were performed for the conversion of the acidic amino acid fractions from sugar beet vinasse and poultry feather meal (Tables S5-S6) into aliphatic C4-C5 diesters and trimethylamine by reductive deamination. For comparison, fermentative produced glutamic acid was considered as a feedstock for that purpose as well (Table S7). To perform these calculations some assumptions were made:

- Quantities of reagents are based on the amounts of reactants consumed as in our manuscript; for 1 mol glutamic acid 2.2 mol formaldehyde, 3 mol methanol and 3 mol H_2 are consumed or for 1 ton glutamic acid 450 kg formaldehyde, 650 kg methanol and 42 kg H_2 are consumed (Table S7). However, as aspartic acid comes together with glutamic acid an additional amount of formaldehyde, methanol and H_2 is required (Tables S5-S6).
- Quantities of products correspond to the highest yields obtained in the article; 81% dimethyl glutarate, 99% dimethyl succinate and > 99% TMA.
- The price of aspartic acid equated to 0 €/ton as it comes together with glutamic acid in the acidic amino acid fraction.
- The price of paraformaldehyde was used instead of formaldehyde; formaldehyde is available in liquid form in an aqueous solution (37 wt%) but paraformaldehyde can be obtained as a solid and will readily form formaldehyde by thermal degradation. In this way, formaldehyde can be added as a gas to the reactor.

Table S4. Protein content, glutamic and aspartic acid content after hydrolysis and prices of selected biomass streams.

Biomass stream	Protein content (%)	Glutamic acid content (%)	Aspartic acid content (%)	Price (€/ton biomass)	Estimated price (€/ ton protein)
DDGS[9,10,8,11]	20-40	25-30	5	130-150	500
Sugar beet vinasse[10,8]	15-30	55	8	150-180	700
Castor bean meal[12,13]	30-60	20	10	100-130	300
Soy bean meal[11]	45-55	20	12	300	600
Poultry feather meal[10,8,14]	80-90	10	7	300	350

Table S5. Economic feasibility calculation concerning the use of sugar beet vinasses for the production of dimethyl glutarate and trimethylamine from glutamic acid.

Reagents	Price (€/ton)	Quantity (kg/ton Glu) [a]	Price (€/ton Glu)	Products	Price (€/ton)	Quantity (kg/ton Glu) [a]	Price (€/ton Glu)
Glutamic acid	1200	1000	1200	Dimethyl glutarate	2200	880	1950
Aspartic acid	0	130	0	Dimethyl succinate	1500-1800	142	240
Paraformaldehyde	540	500	270	Trimethyl amine	1000	460	460
Methanol	250	715	180	Residual amino acids	> 200	340	70
H_2	1350	46	62				
Total			**1712**				**> 2720**

[a] Quantities are based on the amount of reactant consumed and the corresponding product yields as obtained in this article.

Table S6. Economic feasibility calculation concerning the use of poultry feather meal for the production of dimethyl glutarate and trimethylamine from glutamic acid.

Reagents	Price (€/ton)	Quantity (kg/ton Glu) [a]	Price (€/ton Glu)	Products	Price (€/ton)	Quantity (kg/ton Glu) [a]	Price (€/ton Glu)
Glutamic acid	2860	1000	2860	Dimethyl glutarate	2200	880	1950
Aspartic acid	0	500	0	Dimethyl succinate	1500-1800	550	900
Paraformaldehyde	540	700	380	Trimethyl amine	1000	620	620
Methanol	250	1000	250	Residual amino acids	> 300	8500	2550
H_2	1350	63	85				
Total			**3575**				**> 6020**

[a] Quantities are based on the amount of reactant consumed and the corresponding product yields as obtained in this article.

Glutamic acid obtained by fermentation

Table S7. Economic feasibility calculation concerning the use of fermentative derived glutamic acid for the production of dimethyl glutarate and trimethylamine.

Feed	Price (€/ton)	Quantity (kg/ton Glu) [a]	Price (€/ton Glu)	Products	Price (€/ton)	Quantity (kg/ton Glu) [a]	Price (€/ton Glu)
Glutamic acid	1200	1000	1200	Dimethyl glutarate	2200	880	1950
Paraformaldehyde	540	450	243	Trimethyl amine	1000	400	400
Methanol	250	650	163				
H_2	1350	42	57				
Total			**1663**				**2350**

[a] Quantities are based on the amount of reactant consumed and the corresponding product yields as obtained in this article.

It has to be noted that catalyst cost and operating costs are not included in these calculations. However, the price-gap between the reagents and the products is large enough and provides industrial opportunities, certainly for the valorization of protein waste. The Pt/TiO_2 can be easily recycled and reused (Figure 7). Moreover, platinum group metals are not wasted but recycled from deactivated catalysts by catalyst manufacturers. This will end up in a platinum cycle between the manufacturer and the end user, and the high cost of platinum should therefore rather be considered as an investment cost. On the other hand, operating costs for performing reductive deamination of glutamic acid above 200 °C can be reasonable, due to the favorable thermodynamics. Thermodynamic calculations for the reductive N-alkylation and C-N hydrogenolysis were performed for simplicity with monomethylamine, trimethylamine, diethylamine and triethylamine as their data are readily available:

Reductive alkylation:

$MMA + 2\ HCHO + 2\ H_2 \rightarrow TMA + 2\ H_2O$ reaction enthalpy: -253.4 kJ/mol

The highly exothermic nature of the above reaction is mainly due to the formation of water.

C-N hydrogenolysis:

$TMA + H_2 \rightarrow CH_4 + DMA$ reaction enthalpy: -70 kJ/mol (gas)

$(C_2H_5)_2NH + H_2 \rightarrow C_2H_6 + C_2H_5NH_2$ reaction enthalpy: -58 kJ/mol (gas)

$(C_2H_5)_3N + H_2 \rightarrow C_2H_6 + (C_2H_5)_2NH$ reaction enthalpy: -57 kJ/mol (gas)

From these 3 different C-N hydrogenolysis reactions it can be concluded that the reaction enthalpy of the C-N hydrogenolysis reaction of dimethyl *N*,*N*-dimethyl glutamate will be around -60 kJ/mol.

So the overall reaction sequence (sum of both reactions) results in -310 kJ/mol. This energy corresponds to the released heat during both reactions and can be used to heat up the reactor feed. If in an ideal scenario the reaction can be performed at a concentration of 0.5 M, for 1 mol *N*,*N*-dimethyl glutamate, 2 liters of feed (mainly methanol)

have to be heated up to 200 °C, requiring 780 kJ based on the tabulated heat capacity for methanol. Consequently, by using an efficient heat exchanger (> 60%), the overall released reaction heat can be sufficient to maintain the desired reaction temperature.

Finally, expensive distillation strategies to separate dimethyl glutarate (T_{bp} = 214 °C) and dimethyl succinate (T_{bp} = 196 °C) can be avoided, because they can be used as blends for the synthesis of alkyd resins or as green solvent.

In conclusion, the large price-gap between the (renewable) feedstock and the output, the use of a reusable heterogeneous catalyst, the favorable thermodynamics and the prevention of any waste products is very promising for a sustainable process to convert glutamic acid into dimethyl glutarate and TMA.

1 W. R. Bowman, *J. Chem. Soc.*, 1950, 1342–1345.

2 J. T. Scanlon and D. E. Willis, *J. Chromatogr. Sci.*, 1985, **23**, 333–340.

3 A. D. Jorgensen, K. C. Picel and V. C. Stamoudis, *Anal. Chem*, 1990, **62**, 683–689.

4 K. Schofield, *Prog. Energy Combust. Sci.*, 2008, **34**, 330–350.

5 C. L. Faiola, M. H. Erickson, V. L. Fricaud, B. T. Jobson and T. M. Vanreken, *Atmos. Meas. Tech.*, 2012, **5**, 1911–1923.

6 J. R. Copeland, I. A. Santillan, S. M. Schimming, J. L. Ewbank and C. Sievers, *J. Phys. Chem. C*, 2013, **117**, 21413–21425.

7 Biofuels Research Advisory Council, *Biofuels in the European Union - A vision for 2006 and beyond*, 2006.

8 W. Mulder, B. Van den Broek, J. Sanders, M. Bruins and E. Scott, *Biobased economy: de potentie van eiwitten voor technische toepassingen*, 2012.

9 R. L. Belyea, K. D. Rausch and M. E. Tumbleson, *Bioresour. Technol.*, 2004, **94**, 293–298.

10 T. M. Lammens, M. C. R. Franssen, E. L. Scott and J. P. M. Sanders, *Biomass and Bioenergy*, 2012, **44**, 168–181.

11 W. Mulder, *Proteins in Biomass Streams*, 2010.

12 R. S. Lacerda, A. M. Q. B. Bittante, H. Chambi, C. A. Gomide, I. C. F. Moraes, R. A. de Carvalho and P. J. do Amaral Sobral, 2011, p. 6.

13 C. Martín, A. Moure, G. Martín, E. Carrillo, H. Domínguez and J. C. Parajó, *Biomass and Bioenergy*, 2010, **34**, 533–538.

14 P. G. Dalev, *Bioresour. Technol.*, 1994, **48**, 265–267.